

Supplemental Methods

Bulk samples of Tarawera tephra were analysed by X-ray Fluorescence (XRF) using standard techniques at Washington State University GeoAnalytical Laboratory as described by Rowe et al. (2012). Due to the scarcity of crystal cargo within the basaltic scoria, large samples ($\geq 1000 \mu\text{m}$) were crushed and sieved until all material ranged in size from 250-710 μm . The majority of groundmass was magnetically separated and stored, while the remainder was picked through under a binocular microscope. All major minerals were sorted and separated, then mounted in epoxy for microanalysis.

Mineral grains and melt inclusions were analysed by electron microprobe in the Washington State University GeoAnalytical Lab using a JEOL 8500F field emission microprobe. Olivine grains were analysed using a 15 KeV accelerating voltage, 50 nA beam current and focused beam. Plagioclase, pyroxene, and melt inclusions were analysed using a 15 KeV accelerating voltage, 30 nA beam current and 5 μm beam.

Inclusions are primarily circular to ellipsoid, typically ranging in size from 10 to 50 μm but are typically below 20 μm in clinopyroxene. Only glassy melt inclusions were analysed to avoid significant post-entrapment correction complications. However, vapour bubbles were present in many of the inclusions. Data on size or volume proportion of vapour bubbles is limited (student data collection from 2011-2012); although not present in all melt inclusions, vapour bubbles range up to $\sim 15 \mu\text{m}$ in diameter. Barker et al (2020) correct major element compositions of olivine-hosted melt inclusions for post-entrapment crystallization and Fe-loss using Petrolog (Danyushevsky and Plechov 2011). New clinopyroxene-hosted melt inclusions are corrected for post-entrapment crystallization only, using the reverse crystallization application of Petrolog, with clinopyroxene-melt equilibria constrained by Langmuir et al (1992). Reverse crystallization progressed until the calculated fractionating clinopyroxene composition had an Mg# equivalent to the measured clinopyroxene Mg#. Mineral-melt equilibria was confirmed using the procedure outlined by Putirka (2008) based on predicted versus measured DiHd (Diopside-Hedenbergite) and EnFs (Enstatite-Ferrosilite) components, and a clinopyroxene-melt $KD_{\text{Fe-Mg}}$ of 0.28 (Putirka et al., 1996; Putirka, 1999).

TIMS Sr isotope measurements

The chemical separation for bulk feldspar and the isotopic measurements were performed at Miami University. The feldspar separate samples were washed in a mixture of HCl and HF following methods described in Carlson et al. (2004), dried and spiked with ^{84}Sr and ^{87}Rb spikes to enable the determination of elemental composition. The feldspar separates with the spikes were then dissolved overnight in capped Teflon beakers on a hotplate in a 2 to 1 mixture of concentrated HF and HNO_3 acids. The sample was dried and prepared for Rb and Sr separation following methods described by Walker et al. (1989). Samples were dissolved in a mixture of diluted HCl and HF and were loaded onto cation exchange resin. Sr cut was collected, dried and prepared for clean-up columns. The Rb fraction was ready to be analyzed after collection and drying. The Rb concentration of the feldspar separates was determined on ICP-MS by comparing the sample values with a Rb standard following the method described by Waight et al. (2002). The isotopic composition of the feldspar separates were measured on a Finnigan Triton Thermal Ionization Mass Spectrometry. Sr was corrected for mass fractionation using $^{86}\text{Sr}/^{88}\text{Sr} = 0.1194$ and reported relative to NBS 987 standard value of $^{87}\text{Sr}/^{86}\text{Sr} = 0.71025$.

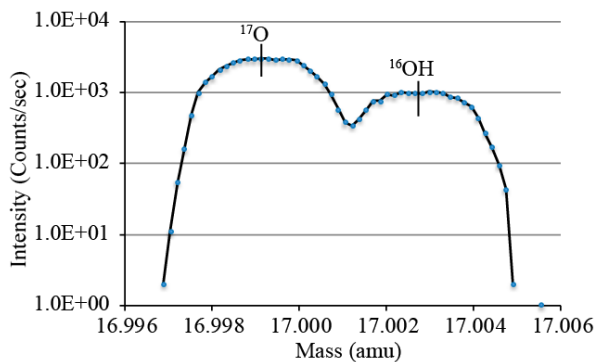
MC-ICPMS Sr isotope measurements

Sr isotopic ratios were determined via the use of a New Wave UP-213 Nd-YAG laser coupled to a ThermoFinnigan Neptune MC-ICPMS in the GeoAnalytical Laboratory at Washington State University using methods identical to Wolff et al. (2011) based upon Ramos et al. (2004). Plagioclase grains were separated and mounted in epoxy, polished prior to analysis. Laser power was varied throughout the analysis period to maintain a fluence of 11-13 J/cm^2 and prior to each analysis an on-peak baseline was performed. Laser troughs were 80 μm wide and >600 μm in length allowing for the 100 isotope ratios used to determine the final $^{87}\text{Sr}/^{86}\text{Sr}$ ratio to be gathered in two passes over the sample with the stage raised approximately 2 microns between passes. Speed of passes was 30 $\mu\text{m}/\text{second}$ and the sample surface was cleaned prior to analysis by a pre-ablation pass before data collection began. In-house standards of plagioclase from the Imnaha Member of the Columbia River Basalts and a plagioclase from the Snake River Plain were used throughout the analysis period with known $^{87}\text{Sr}/^{86}\text{Sr}$ values determined via column chemistry of 0.70405 and 0.70671 respectively. The isotopes measured were ^{83}Kr , ^{84}Sr , ^{85}Rb , ^{86}Sr , ^{87}Sr and ^{88}Sr . The ^{88}Sr is used to determine the mass fractionation between ^{86}Sr and ^{88}Sr (known ratio of 0.1194), the degree of mass fractionation between isotopes is used to correct the known ratio between ^{85}Rb and ^{87}Rb and so derive the abundance of ^{87}Rb . The value of ^{87}Rb was then subtracted

from the overall abundance of mass 87 to derive the ^{87}Sr . No correction was made for the potential contributions from doubly-charged Er and Yb due to their low abundance in plagioclase. Uncertainties on $^{87}\text{Sr}/^{86}\text{Sr}$ laser measurements are 1 standard error of within run uncertainty and uncertainty on standards.

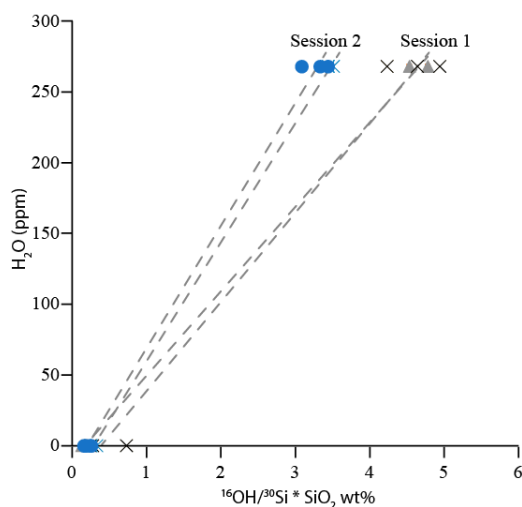
Water in clinopyroxene

Clinopyroxenes embedded in CrystalbondTM were individually polished. After removal of the adhesive, they were remounted in indium for hydrogen analysis. Hydrogen concentrations in



Supplemental Figure 4: High mass resolving power during ^{16}OH analysis of clinopyroxenes, demonstrating ability to distinguish the ^{16}OH peak from the ^{17}O peak.

clinopyroxene were measured by secondary ion mass spectrometry (SIMS) (Cameca 6f) at Arizona State University in collaboration with Rick Hervig over two analytical sessions. Analyses were conducted using a Cs^+ primary ion source, charge balanced with an electron gun, and negative secondary ions were collected at high mass resolving power (~5000 MRP). The high mass resolving power was necessary to distinguish the ^{16}OH peak from the ^{17}O peak (Supplemental Fig. 4). A 100 μm field aperture was placed to allow only secondary ions originating from a circular area 8 μm in diameter in the centre of a defocused 30 μm sputtered crater reduced surface contamination. In addition, a 360 s pre-sputter minimized contribution of volatiles from the sample surface.



Supplemental Figure 5: Calibration curves for determining water contents of clinopyroxenes based on the analysis of PMR-53 (Bell and Ihinger, 2000) for the two analytical sessions.

clinopyroxene were measured by secondary ion mass spectrometry (SIMS) (Cameca 6f) at Arizona State University in collaboration with Rick Hervig over two analytical sessions. Analyses were conducted using a Cs^+ primary ion source, charge balanced with an electron gun, and negative secondary ions were collected at high mass resolving power (~5000 MRP). The high mass resolving power

In addition to ^{16}OH , we collected ion intensities for ^{12}C , ^{18}O , ^{19}F , and ^{30}Si . ^{12}C and ^{19}F were measured primarily to monitor for sample contamination (either surface or melt inclusions). Clinopyroxene standard PMR-53 (“wet” = 268 ppm H_2O ; “dry” = 0 ppm; Bell and Ihinger, 2000) along with San Carlos olivine (“dry”) were mounted with the unknowns and used to construct a calibration curve (Supplemental Fig. 5) for calculating water concentrations in pyroxene.

Calibration curves based on standard analyses were

re-established after each sample change to accommodate changing background concentrations (~10 ppm blank). Water concentrations in pyroxene were calculated using the silica-normalized ion ratios ($^{16}\text{OH}/^{30}\text{Si} * \text{SiO}_2\text{wt}\%$; Supplemental Fig. 5). Anomalous analyses, as indicated by exceptionally high volatile count rates, or highly variable count rates over the 30 analysis cycles, have been removed from the final dataset as these reflect surface contamination and/or the analysis of heterogeneities within the clinopyroxene grains.

References

- Bell DR, Ihinger PD. 2000. The isotopic composition of hydrogen in nominally anhydrous mantle minerals. *Geochimica et Cosmochimica Acta*. 64:2109-2118.
- Carlson RW, Irving AJ, Schulze DJ, Hearn Jr. BC. 2004. Timing of Precambrian melt depletion and Phanerozoic refertilization events in the lithospheric mantle of the Wyoming Craton and adjacent Central Plains Orogen. *Lithos*. 77:453-472.
- Danyushevsky LV, Plechov P. 2011. Petrolog3: Integrated software for modelling crystallization processes. *Geochemistry, Geophysics, Geosystems*. 12:Q07021. [Doi.org/10.1029/2011GC003516](https://doi.org/10.1029/2011GC003516).
- Langmuir CH, Klein EM, Plank T. 1992. Petrologic systematics of mid-ocean ridge basalts: Constraints on melt generation beneath ocean ridges. *Mantle flow and melt generation at mid-ocean ridges*. 71:183-280.
- Putirka KD. 1999. Clinopyroxene+liquid equilibrium to 100 kbar and 2450 K. *Contributions to Mineralogy and Petrology*. 135:151-163.
- Putirka KD. 2008. "Thermometers and Barometers for Volcanic Systems." *Reviews in Mineralogy and Geochemistry* 69 (1):61–120. <https://doi.org/10.2138/rmg.2008.69.3>.
- Putirka K, Johnson M, Kinzler R, Walker D. 1996. Thermobarometry of mafic igneous rocks based on clinopyroxene-liquid equilibria, 0.30 kbar. *Contributions to Mineralogy and Petrology*. 123:92-108.
- Ramos FC, Wolff JA, Tollstrup DL. 2004. Measuring $^{87}\text{Sr}/^{86}\text{Sr}$ variations in minerals and groundmass from basalts using LA-MC-ICPMS. *Chemical Geology*. 211:135-158.
- Rowe MC, Ellis BS, Lindeberg. 2012. Quantifying crystallization and devitrification of rhyolites by means of X-ray diffraction and electron microprobe analysis. *American Mineralogist*. 97:1685-1699.
- Waight T, Baker J, Willigers B. 2002. Rb isotope dilution analyses by MC-ICPMS using Zr to correct for mass fractionation: towards improved Rb – Sr geochronology? *Chemical Geology* 186:99-116.
- Walker RJ, Carlson RW, Shirey SB, Boyd FR. 1989. Os, Sr, Nd, and Pb isotope systematics of southern African peridotite xenoliths: Implications for the chemical evolution of subcontinental mantle. *Geochimica et Cosmochimica Acta*. 53:1583-1595.
- Wolff JA, Ellis BS, Ramos FC. 2011. Strontium isotopes and magma dynamics: insights from high-temperature rhyolites. *Geology*. 39:931-934.